

# Graphene/GaN Schottky diodes: Stability at elevated temperatures

S. Tongay,<sup>1,2,3,a)</sup> M. Lemaître,<sup>2</sup> T. Schumann,<sup>1</sup> K. Berke,<sup>1</sup> B. R. Appleton,<sup>2,3</sup> B. Gila,<sup>2,3</sup> and A. F. Hebard<sup>1,b)</sup>

<sup>1</sup>Department of Physics, University of Florida, Gainesville Florida 32611, USA

<sup>2</sup>Material Science and Engineering, University of Florida, Gainesville, Florida 32611, USA

<sup>3</sup>Nanoscience Institute for Medical and Engineering Technology, University of Florida, Gainesville, Florida 32611, USA

(Received 12 May 2011; accepted 12 July 2011; published online 7 September 2011)

Rectification and thermal stability of diodes formed at graphene/GaN interfaces have been investigated using Raman Spectroscopy and temperature-dependent current-voltage measurements. The Schottky barriers formed between GaN and mechanically transferred graphene display rectification that is preserved up to 550 K with the diodes eventually becoming non-rectifying above 650 K. Upon cooling, the diodes show excellent recovery with improved rectification. We attribute these effects to the thermal stability of graphene, which acts like an impenetrable barrier to the diffusion of contaminants across the interface, and to changes in the interface band alignment associated with thermally induced dedoping of graphene. © 2011 American Institute of Physics. [doi:10.1063/1.3628315]

Graphene has been studied intensively since becoming experimentally accessible via techniques such as mechanical exfoliation, thermal decomposition, and chemical vapor deposition (CVD).<sup>1–5</sup> Graphene's high electron mobility, outstanding optical properties, and chemical and mechanical stability<sup>1</sup> make it ideal for analog devices such as metal-semiconductor field effect transistors (MESFETs) and high-electron mobility transistors (HEMTs).<sup>6–12</sup> Unlike metal-oxide-semiconductor field effect transistors (MOSFETs), MESFETs, and HEMTs do not involve an insulating oxide layer; instead the switching is obtained at metal-semiconductor (Schottky) junctions.<sup>13</sup> A major concern for MESFETs and HEMTs is the need for thermally stable metal contacts that can survive local overheating effects when the device is in operation.<sup>14</sup> Thermally and mechanically stable graphene and multi-layer graphene (MLG) contacts are good candidates for replacing conventional metal contacts, which degrade easily at high temperatures by diffusing into the semiconductor and irreversibly forming undesirable ohmic contacts.

Here, we report on rectification at graphene (or MLG)/GaN junctions. We observe (1) the stable operation of graphene-based diodes formed on GaN up to 550 K, (2) leaky reverse-bias characteristics above 600 K, eventually resulting in non-rectifying behavior, and (3) enhanced room-temperature rectification accompanied by diminished reverse-bias leakage following prolonged annealing at 900 K. We attribute the observed temperature stability to the exceptionally robust thermal properties of graphene; temperatures of 900 K are not high enough to break carbon-carbon bonds and the interstitial voids in the honeycomb lattice are small enough to prevent diffusion of most contaminants across the interface. Improvement in the post-anneal characteristics are attributed to anneal-induced removal of impurities/dopants at the interface, a decrease in the ideality

constant toward unity, and changes in the band alignment at the interface due to shifts in graphene's Fermi level as corroborated by Raman measurements.

We used commercially available *n*-type GaN doped with Si ( $1 \times 10^{16} \text{ cm}^{-3}$ ). Prior to the device fabrication, the GaN wafers were thoroughly cleaned by successive immersions into acetone, ethanol, and 1:10 HCl:H<sub>2</sub>O. Ohmic contacts were made on GaN using conventional recipes.<sup>15</sup> After ohmic contact formation, 0.5-1  $\mu\text{m}$ -thick SiO<sub>x</sub> and Cr(1 nm)/Au(100 nm) window frames ( $\sim 1000 \mu\text{m}$ - $2000 \mu\text{m}$  squares) were grown onto GaN. Here, the insulating SiO<sub>x</sub> layer prevents the Cr/Au contacts from forming Schottky diodes while the Cr/Au layer provides electrical contact to the overlying graphene sheets (Fig. 1). Annealing of Au thin films deposited onto SiO<sub>2</sub> is known to cause agglomeration and even Au diffusion into the SiO<sub>2</sub> at temperatures well above the Au/Si eutectic temperature ( $\sim 650 \text{ K}$ ) leaving conductive Au/SiO<sub>2</sub> interface. Prior to the graphene transfer, we find

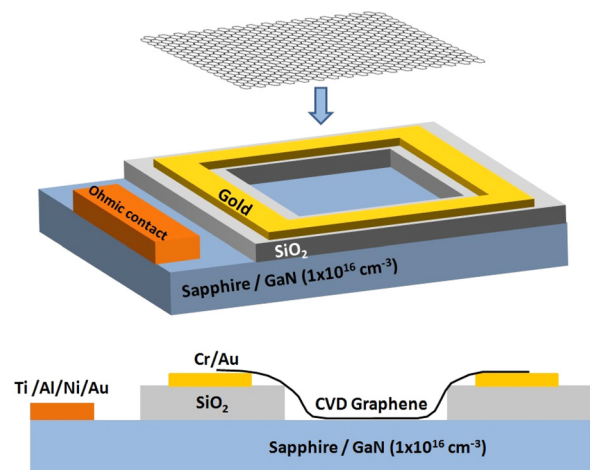


FIG. 1. (Color online) Top and side views of the sample geometry. The arrow indicates mechanical transfer of the graphene counter-electrode onto the predeposited Cr/Au contact pad and the pristine GaN surface. (b) Side view of the device.

<sup>a)</sup>Electronic mail: afh@phys.ufl.edu.

<sup>b)</sup>Author to whom correspondence should be addressed. Electronic mail: tongay@phys.ufl.edu.

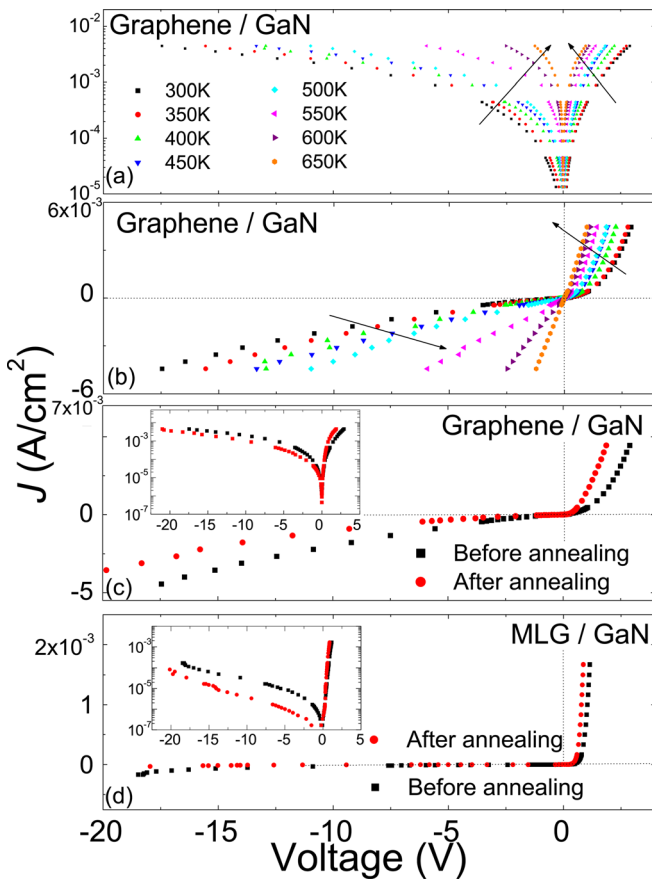


FIG. 2. (Color online)  $J$ - $V$  characteristics of graphene/ $n$ -GaN diodes from 300 K up to 650 K in (a) semi-logarithmic scale and (b) linear scale. Black arrows indicate increasing temperature. Room temperature  $J$ - $V$  characteristics of (c) graphene/ $n$ -GaN and (d) MLG/ $n$ -GaN diodes measured upon cooling from 900 K. Inset: Post annealing  $J$ - $V$  characteristics on a semilogarithmic scale.

that the devices are open circuit before and after the annealing. Upon transferring the graphene, the devices show rectification and reliable electrical connection to the graphene is maintained with robust Au or carbon paint contacts during subsequent anneals.

The graphene sheets were grown on Cu and Ni foils using conventional methods.<sup>4,16</sup> The graphene sheets, identified by Raman spectroscopy, displayed a large 2D to G intensity ratio ( $I_{2D}/I_G \geq 2$ ) and a low D peak (Fig. 3(a)). Samples were annealed in a quartz tube furnace under  $10^{-3}$ – $10^{-6}$  Torr pressure and electrical characteristics were measured *in-situ* using a voltage-current source meter.

In Figs. 2(a) and 2(b), we show the current density ( $J$ ) measured across the graphene/GaN interface as a function of applied bias ( $V$ ) from room temperature up to 650 K. The  $J$ - $V$  measurements show good rectification in the  $-21$  V to 2.5 V range for temperatures in the range 300–550 K. However, above 550 K, the diodes start leaking in reverse bias and become non-rectifying above 650 K. Electron transport across the Schottky barrier is well described by thermionic emission theory, i.e., the Richardson equation,

$$J = J_s(T)[\exp(qV/\eta k_B T) - 1], \quad (1)$$

where  $J_s = A^* T^2 \exp(-q\phi_{SBH}/k_B T)$  is the saturation current density,  $q\phi_{SBH}$  is the Schottky barrier height (SBH),  $A^*$  is the

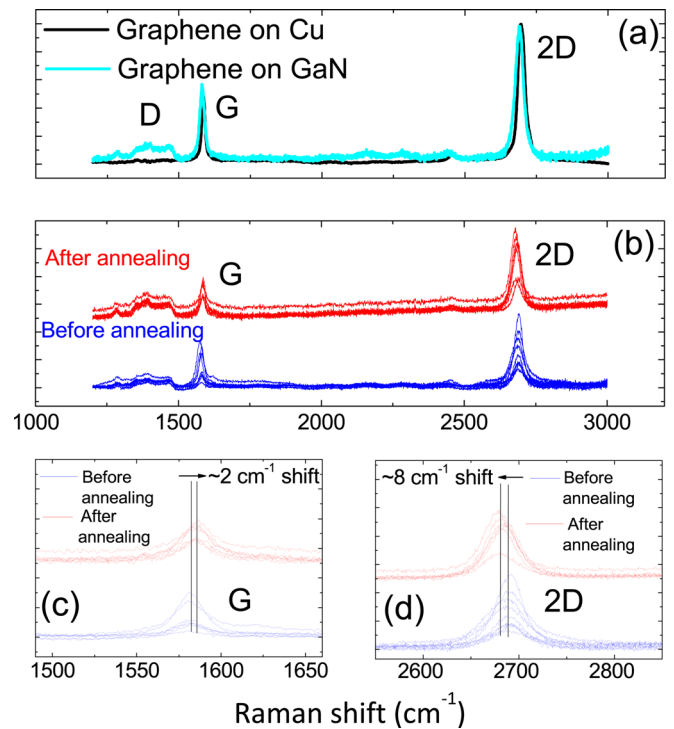


FIG. 3. (Color online) (a) Raman spectrum taken on graphene grown on Cu foils (black) and after transferring onto GaN (cyan) (b) Raman spectrum of graphene on GaN before (green) and after (red) annealing in 1200–3000  $\text{cm}^{-1}$  range taken on random spots on the device. Zoomed G and 2D peak regions are plotted in (c) and (d), respectively.

Richardson constant,  $T$  is the absolute temperature,  $\eta$  is the ideality factor, and  $V$  is the applied voltage.<sup>13</sup> Equation (1) explains the increase in  $J$  with increasing temperature (see arrows of Figs. 2(a) and 2(b)) in the forward bias region where  $V < \phi_{SBH}$  and in the reverse bias region where  $V$  is negative. At high enough temperatures, electrons have enough energy to overcome the barrier in both directions and the rectification disappears.

Although our diodes become non-rectifying in the 650–700 K temperature range, they survive prolonged (2 days) anneals at 900 K with full recovery and improved characteristics (Figs. 2(c) and 2(d)) when subsequently cooled down to room temperature. We note that the graphene/GaN junctions display leakier reverse bias characteristics compared to MLG/GaN junctions. This excess leakage in reverse bias can be attributed to a voltage induced increase in graphene's Fermi level accompanied by a corresponding decrease in  $\phi_{SBH}$ . Fermi level pinning prevents this excess leakage in MLG/GaN junctions as shown in Fig. 2(d). After annealing, graphene (or MLG)/GaN diodes not only show excellent recovery but also display improved rectification with increased  $J_{for}$  and decreased  $J_{rev}$  compared to pre-annealed samples. Recovery of the graphene/GaN diodes suggests that the diffusion of  $sp^2$  bonded carbon atoms into GaN is energetically unfavorable and that there is no diffusion of contaminants through the graphene interface. Here, we note that various impurities originating from chemicals used to release graphene sheets from Cu/Ni exist at the graphene/GaN interface. The decrease in  $J_{rev}$  might be attributed to the anneal-induced removal of residue on the graphene sheets and the removal of impurities at the graphene/GaN interface

accompanied by a reduction of tunneling and/or non-thermionic emission current components. A closer look at the forward bias characteristics shows that  $J_s$  increases and  $\eta$  decreases by 20%–30%, i.e., approaches unity, which is again consistent with the removal of impurities. Since  $J_s$  is sensitive to the SBH, the increase in  $J_s$  implies that the SBH is lowered after annealing and, therefore,  $J_{for}$  is increased in conjunction with the improvement in  $\eta$ . Using Eq. (1), we estimate the SBH ( $\eta$ ) of the diodes as  $\phi_{SBH} \sim 0.74$  eV ( $\eta \sim 2.9$ ) before annealing and  $\phi_{SBH} \sim 0.70$  eV ( $\eta \sim 2.4$ ) after annealing. These experiments have been repeated on 4 graphene/GaN and 6 MLG/GaN samples with similar results.

Although the anneal-induced increase in  $J_s$  for fixed forward bias voltages implies that the SBH is lowered, it does not provide a physical mechanism describing how this decrease is obtained. Some insight is gained by examining theories based on interacting (bond polarization, Schottky-Mott) and non-interacting (Bardeen) models described in the literature.<sup>17</sup> While most semiconductors fall between the Schottky-Mott and Bardeen limit, wide band-gap semiconductors mostly obey the Schottky-Mott model.<sup>18</sup> Regardless, both models correlate the SBH to the metal's workfunction ( $\Phi_M$ ). Due to graphene's low electron density, any charge transfer between carbon and coexisting dopants can alter graphene's workfunction ( $\Phi_G$ ). The effect of doping on the G and 2D peak position and linewidth has been reported and correlated to changes in  $\Phi_G$ .<sup>19,20</sup> Following similar methods, we have measured the Raman spectra of graphene deposited on GaN both before and after annealing. The Raman spectra of CVD-prepared graphene on Cu and GaN are shown in Fig. 3(a). Because of sample handling during the transfer processes, the D peak intensity becomes observable. Raman spectra measured at different regions of the contact area before (green) and after (red) annealing in the 1200–3000  $\text{cm}^{-1}$  wave number range (Figs. 3(b)–3(d)) capture the G and 2D peaks. After annealing, the G peak shifts from  $1582.3 \pm 2$  to  $1584.4 \pm 2$   $\text{cm}^{-1}$  (Fig. 3(c)) and the 2D peak shifts from  $2688.5 \pm 1$  to  $2680.7 \pm 2$   $\text{cm}^{-1}$  (Fig. 3(d)). These peak position shifts imply that the concentration of *p*-dopants is diminished and the Fermi level increases as  $\Phi_G$  decreases.<sup>20</sup> According to the Schottky-Mott model, the SBH can be correlated to the metal work function as,  $\phi_{SBH} = \Phi_G - e\chi_{GaN}$ , and the decrease in  $\Phi_G$  can be associated with our observed decrease in the SBH as discussed in the preceding paragraph.

To summarize, we have demonstrated the formation of graphene and MLG based diodes on GaN substrates and have studied the temperature stability from 300 K up to 900 K. We have shown that graphene/GaN diodes operate stably up to 550 K and above 650 K become non-rectifying. Further

annealing of samples to 900 K for up to two days does not cause permanent degradation, rather the diodes when cooled to room temperature improve in quality and become more rectifying. The anneal-induced increase in rectification is attributed to a reduction of the effect of impurities and residue, improvement in  $\eta$ , and a decrease in  $\Phi_G$  which lowers the Schottky barrier height at both the graphene/GaN and MLG/GaN interface. Our observation of robust temperature stability of high quality graphene/GaN Schottky diodes promises integration of graphene into high-performance analog devices operating at elevated temperatures.

This work is supported by the Office of Naval Research (ONR) under Contract Number 00075094 (BA) and by the National Science Foundation (NSF) under Contract Number 1005301 (AFH).

- <sup>1</sup>K. S. Novoselov, A. K. Geim, S. V. Morozov, D. Jiang, Y. Zhang, S. V. Dubonos, I. V. Grigorieva, and A. A. Firsov, *Science* **306**, 666 (2004).
- <sup>2</sup>C. Berger, Z. Song, T. Li, X. Li, A. Y. Ogbazghi, R. Feng, Z. Dai, A. N. Marchenkov, E. H. Conrad, P. N. First, and W. A. de Heer, *J. Phys. Chem.* **108**, 19912 (2004).
- <sup>3</sup>X. Li, W. Cai, J. An, S. Kim, J. Nah, D. Yang, R. Piner, A. Velamakanni, I. Jung, E. Tutuc, S. K. Banerjee, L. Colombo, and R. S. Ruoff, *Science* **324**, 1312 (2009).
- <sup>4</sup>K. S. Kim, Y. Zhao, H. Jang, S. Y. Lee, J. M. Kim, K. S. Kim, J. Ahn, P. Kim, J. Choi, and B. H. Hong, *Nature* **457**, 706 (2009).
- <sup>5</sup>P. W. Sutter, J. I. Flege, and E. A. Sutter, *Nature Mater.* **7**, 406411 (2008).
- <sup>6</sup>K. Chung, C. Lee, and G. Yi, *Science* **330**, 655657 (2010).
- <sup>7</sup>Y. Ye, L. Gan, L. Dai, Y. Dai, X. Guo, H. Meng, B. Yu, Z. Shi, K. Shang, and G. Qin, *Nanoscale* **3**, 1477 (2011).
- <sup>8</sup>X. Li, H. Zhu, K. Wang, A. Cao, J. Wei, C. Li, Y. Jia, Z. Li, X. Li, and D. Wu, *Adv. Mater.* **22**, 2743 (2010).
- <sup>9</sup>Th. Seyller, K. V. Emtsev, F. Speck, K.-Y. Gao, and L. Ley, *Appl. Phys. Lett.* **88**, 242103 (2006).
- <sup>10</sup>S. Tongay, T. Schumann, and A. F. Hebard, *Appl. Phys. Lett.* **95**, 222103 (2009).
- <sup>11</sup>S. Tongay, T. Schumann, X. Miao, B. R. Appleton, and A. F. Hebard, *Carbon* **49**(6), 2033 (2011).
- <sup>12</sup>P. Avouris, *Nano Lett.* **10**, 42854294 (2010).
- <sup>13</sup>S. M. Sze, *Physics of Semiconductor Devices*, 2nd ed. (Wiley, New York, 1981).
- <sup>14</sup>W. Lim, J. H. Jeong, J. H. Lee, S. B. Hur, J. K. Ryu, K. S. Kim, T. H. Kim, S. Y. Song, J. I. Yang, and S. J. Pearton, *Appl. Phys. Lett.* **97**, 242103 (2010).
- <sup>15</sup>Z. Fan, S. N. Mohammad, W. Kim, O. Aktas, A. E. Botchkarev, and H. Morkoc, *Appl. Phys. Lett.* **68**, 1672 (1996).
- <sup>16</sup>X. Li, C. W. Magnuson, A. Venugopal, J. An, J. W. Suk, B. Han, M. Borysiak, W. Cai, A. Velamakanni, Y. Zhu, L. Fu, E. M. Vogel, E. Voelkl, L. Colombo, and R. S. Ruoff, *Nano Lett.* **10**, 4328 (2010).
- <sup>17</sup>R. T. Tung, *Mater. Sci. Eng. R.* **35**, 1 (2001).
- <sup>18</sup>C. Lu and S. N. Mohammad, *Appl. Phys. Lett.* **89**, 162111 (2006).
- <sup>19</sup>J. Yan, Y. Zhang, P. Kim, and A. Pinczuk, *Phys. Rev. Lett.* **98**, 166802 (2007).
- <sup>20</sup>A. Das, S. Pisana, B. Chakraborty, S. Piscanec, S. K. Saha, U. V. Waghmare, K. S. Novoselov, H. R. Krishnamurthy, A. K. Geim, A. C. Ferrari, and A. K. Sood, *Nature Nanotechnol.* **3**, 210 (2008).